

Metabolic Disposition of Triazolam and Clobazam in Humanized CYP3A Mice with a Double-Knockout Background of Mouse *Cyp2c* and *Cyp3a* Genes^[S]

Kaoru Kobayashi, Genki Minegishi, Nina Kuriyama, Atsushi Miyajima, Satoshi Abe, Kanako Kazuki, and Yasuhiro Kazuki

Department of Biopharmaceutics, Graduate School of Clinical Pharmacy, Meiji Pharmaceutical University, Kiyose, Japan (K.Ko., G.M., N.K., A.M.) and Chromosome Engineering Research Center (CERC) (S.A., K.Ka., Y.K.) and Department of Chromosome Biomedical Engineering, School of Life Science, Faculty of Medicine (Y.K.), Tottori University, Tottori, Japan

Received August 18, 2022; accepted November 3, 2022

ABSTRACT

Knockout (KO) of mouse *Cyp3a* genes increases the expression of hepatic CYP2C enzymes, which can metabolize triazolam, a typical substrate of human CYP3A. There is still marked formation of 1'-hydroxytriazolam in *Cyp3a*-KO (3aKO) mice after triazolam dosing. Here, we generated a new model of humanized CYP3A (hCYP3A) mice with a double-KO background of *Cyp3a* and *Cyp2c* genes (2c3aKO), and we examined the metabolic profiles of triazolam in wild-type (WT), 2c3aKO, and hCYP3A/2c3aKO mice *in vitro* and *in vivo*. *In vitro* studies using liver microsomes showed that the formation of 1'-hydroxytriazolam in 2c3aKO mice was less than 8% of that in WT mice. The formation rate of 1'-hydroxytriazolam in hCYP3A/2c3aKO mice was eightfold higher than that in 2c3aKO mice. *In vivo* studies showed that area under the curve (AUC) of 1'-hydroxytriazolam in 2c3aKO mice was less than 3% of that in WT mice. The AUC of 1'-hydroxytriazolam in hCYP3A/2c3aKO mice was sixfold higher than that in 2c3aKO mice. These results showed that formation of 1'-hydroxytriazolam was significantly decreased in 2c3aKO mice. Metabolic functions of

human CYP3A enzymes were distinctly found in hCYP3A mice with the 2c3aKO background. Moreover, hCYP3A/2c3aKO mice treated with clobazam showed human CYP3A-mediated formation of desmethylclobazam and prolonged elimination of desmethylclobazam, which is found in poor metabolizers of CYP2C19. The novel hCYP3A mouse model without mouse *Cyp2c* and *Cyp3a* genes (hCYP3A/2c3aKO) is expected to be useful to evaluate human CYP3A-mediated metabolism *in vivo*.

SIGNIFICANT STATEMENT

Humanized CYP3A (hCYP3A/2c3aKO) mice with a background of double knockout (KO) for mouse *Cyp2c* and *Cyp3a* genes were generated. Although CYP2C enzymes played a compensatory role in the metabolism of triazolam to 1'-hydroxytriazolam in the previous hCYP3A/3aKO mice with *Cyp2c* genes, the novel hCYP3A/2c3aKO mice clearly showed functions of human CYP3A enzymes introduced by chromosome engineering technology.

Introduction

Cytochrome P450 (P450) enzymes constitute gene families that are involved in the metabolism of lipophilic compounds, including therapeutic agents. Since CYP2 and CYP3 families catalyze the metabolism of numerous drugs, they are considered to be clinically relevant (Zanger and Schwab, 2013). Four P450 isoforms (3A4/3A5/3A7/3A43) exist in the human CYP3 family. CYP3A4, which is highly expressed in hepatocytes and intestinal enterocytes, plays important roles in the first-pass metabolism of orally administered drugs. On the other hand, the mouse CYP3 family has eight isoforms (3A11/3A13/3A16/3A25/3A41/3A44/

3A57/3A59). Mouse CYP3A11, CYP3A25, and CYP3A41 are predominantly expressed in the liver, whereas CYP3A13 is detected more in the intestine than in the liver (Martignoni et al., 2006). The species differences in expression profiles of CYP3A isoforms make interspecies comparison complex. Among the CYP2 family, the CYP2C subfamily is the largest and has four isoforms in humans and 15 isoforms in mice. Because of these significant species differences, it is difficult to extrapolate mouse *in vivo* pharmacokinetic data to the human situation. To resolve this problem, various mouse models (e.g., transgenic mice, humanized mice, and chimera mice with human hepatocytes) were developed (Gonzalez et al., 2015; Bissig et al., 2018; Satoh et al., 2018).

We previously developed fully humanized CYP3A (hCYP3A) mice with the *CYP3A* gene cluster, including four human genes (*CYP3A4*, *CYP3A5*, *CYP3A7*, and *CYP3A43*) with a mouse *Cyp3a* knockout (3aKO) background (Kazuki et al., 2013, 2019). The hCYP3A/3aKO mice carry a human or mouse artificial chromosome (MAC) vector, which contains the entire genomic human CYP3A locus. The hCYP3A/3aKO mice recapitulate tissue- and stage-specific expression of human CYP3A genes and human CYP3A-mediated drug metabolism in the mice. *In vitro* studies using liver microsomes showed that metabolites

This study was supported in part by Platform Project for Supporting Drug Discovery and Life Science Research (Basis for Supporting Innovative Drug Discovery and Life Science Research (BINDS)) from AMED under Grant Number JP21am0101124 (Y.K.), Research Support Project for Life Science and Drug Discovery (BINDS) from AMED under grant number JP22ama121046 (Y.K. and K. Kobayashi), and JST CREST under grant number JPMJCR18S4 (Y.K.).

There are no conflicts of interest.

dx.doi.org/10.1124/dmd.122.001087.

^[S]This article has supplemental material available at dmd.aspetjournals.org.

ABBREVIATIONS: 3aKO, *Cyp3a* knockout; AUC, area under the plasma concentration-time curve; CLB, clobazam; FISH, fluorescence in situ hybridization; GAPDH, glyceraldehyde 3-phosphate dehydrogenase; hCYP3A, humanized CYP3A; KO, knockout; LC-MS/MS, liquid chromatography–tandem mass spectrometry; MAC, mouse artificial chromosome; NCLB, N-desmethylclobazam; P450, cytochrome P450; PCR, polymerase chain reaction; WT, wild type.

of triazolam, a typical substrate of CYP3A, were formed in hCYP3A/3aKO mice and that the formation rate was markedly low in 3aKO mice (Kazuki et al., 2013, 2019). However, *in vivo* studies showed no significant difference in the plasma levels of triazolam and its metabolites, 1'-hydroxytriazolam and 4-hydroxytriazolam, after intravenous administration of triazolam between hCYP3A/3aKO and 3aKO mice (Minegishi et al., 2019). In addition, plasma levels of 1'-hydroxytriazolam were also detectable in 3aKO mice after oral administration of triazolam, although the levels of 4-hydroxytriazolam were much lower (Supplemental Fig. 1). Area under the plasma concentration-time curve (AUC) ratios of metabolite/triazolam were not significantly different between hCYP3A/3aKO and 3aKO mice (Supplemental Table 1). Thus, the formation of 1'-hydroxytriazolam and 4-hydroxytriazolam via enzymes other than CYP3A isoforms in 3aKO mice limits the estimation of human CYP3A-mediated metabolism in hCYP3A/3aKO mice.

It has been reported that 1'-hydroxytriazolam and 4-hydroxytriazolam from triazolam in liver microsomes of 3aKO mice are formed by mouse endogenous CYP2C enzymes (Minegishi et al., 2019). This might be due to compensatory mechanisms by CYP2C enzymes increased in 3aKO mice (van Waterschoot et al., 2008). Therefore, we thought that deletion of mouse endogenous CYP2C enzymes in hCYP3A/3aKO mice might enable the evaluation of human CYP3A functions as an *in vivo* mouse model.

Here, we generated a new model of hCYP3A mice with a double-knockout (KO) background of *Cyp3a* and *Cyp2c* genes (hCYP3A/2c3aKO mice), and the *in vitro* and *in vivo* metabolic profiles of triazolam in wild-type (WT), 2c3aKO, and hCYP3A/2c3aKO mice were investigated. In addition, we compared plasma concentration-time profiles of clobazam (CLB) and N-desmethyl CLB (NCLB) between hCYP3A/3aKO and hCYP3A/2c3aKO mice to examine the roles of CYP3A and CYP2C in the sequential metabolism of CLB.

Materials and Methods

Materials. CLB and NCLB were purchased from Sigma-Aldrich Japan (Tokyo, Japan). Triazolam was purchased from Wako Pure Chemicals (Osaka, Japan). 1'-Hydroxytriazolam and 4-hydroxytriazolam were gifted by Nihon Upjohn Co. (Tokyo, Japan). Pooled human liver microsomes (#452161) were purchased from Corning (Corning, NY). Pooled human intestine microsomes (#H0610.I) were obtained from Sekisui Medical (Tokyo, Japan). Other reagents were purchased commercially.

Animals. C57BL/6 mice (CLEA, Tokyo, Japan) were used as WT mice. The generation and characterization of 3aKO mice and hCYP3A/3aKO mice are described in previous reports (Hashimoto et al., 2013; Kazuki et al., 2013; Hashimoto et al., 2016; Abe et al., 2017). In brief, 3aKO mice lacking the mouse *Cyp3a* gene cluster were generated by mating *Cyp3a13*^{-/-} mice and a *Cyp3a57-59*^{-/-} mice. hCYP3A/3aKO mice were produced by crossing 3aKO mice and transchromosomal mice with an MAC vector containing the entire human CYP3A gene cluster (*CYP3A4*, *CYP3A5*, *CYP3A7*, and *CYP3A43*) with their regulatory regions (promoters and enhancers). *Cyp2c*-KO mice (Scheer et al., 2012) were obtained from Taconic Biosciences (Rensselaer, NY) and crossed with hCYP3A/3aKO mice to produce hCYP3A/2c3aKO mice, which are hCYP3A mice with a double-KO background of *Cyp2c* and *Cyp3a* genes, and 2c3aKO mice, which are double-KO mice of *Cyp2c* and *Cyp3a* genes without the hCYP3A-MAC vector. Generation of hCYP3A/2c3aKO mice was confirmed by fluorescence *in situ* hybridization (FISH) analysis of hCYP3A-MAC and genotyping polymerase chain reaction (PCR) with primers detecting human CYP3A genes and mouse *Cyp3a*KO and *Cyp2c*KO (Kazuki et al., 2013; Supplemental Table 2). All genetically modified mice were backcrossed to the C57BL/6 strain for at least 10 generations. Male mice ranging from 10 to 12 weeks of age were used in the present study. All mice were kept in a temperature-controlled environment with a 12-hour light/dark cycle. The present study was conducted in accordance with the Guidelines for the Care and Use of Laboratory Animals as adopted by the Committee on Animal Research of Tottori University.

FISH Analysis. Cultured lymphocytes were treated with 0.075M KCl for 15 minute and fixed with methanol and acetic acid (3:1). Chromosome spread

specimens were prepared using standard methods. FISH analysis was performed using digoxigenin-labeled mouse minor satellite DNA and biotin-labeled CYP3A-BAC DNA (RP11-757A13) as described previously (Tomizuka et al., 1997). Chromosomal DNA was counterstained with DAPI (Sigma Aldrich, St. Louis, MO). FISH images were captured with a CoolCube1 charge-coupled device camera (MetaSystems GmbH, Altlusheim, Germany) coupled with an AxiolmagerZ2 fluorescence microscope (Carl Zeiss GmbH, Jena, Germany). Images were processed using Isis software (Metasystems).

mRNA Analysis. Livers and small intestines (1-cm segments collected at 10 cm from the pyloric region) were subjected to total RNA extraction by using ISOGEN II (Nippon Gene, Tokyo, Japan). To remove contaminating genomic DNA, total RNA was treated with RNase-free DNase I. First-strand cDNA was synthesized by using a random hexamer and a High-Capacity cDNA Reverse Transcription Kit (Thermo Fisher Scientific, Waltham, MA). The synthesized cDNA was subjected to quantitative PCR by a CFX Connect Real-time System (Bio-Rad Laboratories, Hercules, CA). The mRNA expression levels were determined by using THUNDERBIRD probe qPCR Mix (Toyobo, Osaka, Japan) and TaqMan Gene Expression Assays (Hs00604506_m1 for human CYP3A4, Mm00484110_m1 for mouse CYP3A13, Mm00725580_s1 for mouse CYP2C29, Mm00487224_m1 for CYP1A2, Mm00456591_m1 for CYP2B10, Mm02603337_m1 for UGT1A1, and Mm00440761_m1 for *Mdr1a*; Thermo Fisher Scientific). The mRNA expression levels of glyceraldehyde 3-phosphate dehydrogenase (GAPDH) were detected by 20X Pre-Developed TaqMan Assay Reagent mouse GAPDH (Thermo Fisher Scientific) for normalization.

Protein Analysis. Microsomal fractions were prepared from the liver and small intestine of WT, 3aKO, 2c3aKO, hCYP3A/3aKO, and hCYP3A/2c3aKO mice as described previously (Kazuki et al., 2013; Minegishi et al., 2019). Expression of CYP3A4 protein was examined by western blotting as described previously (Kobayashi et al., 2019). Pooled samples (4 µg) for each group were subjected to analysis with pooled human liver and pooled human intestine microsomes. CYP3A4 and GAPDH proteins (loading control) were detected by LuminoGraph I with CS Analyzer 4 (Atto, Tokyo, Japan).

Triazolam Hydroxylation Activity *In Vitro*. An incubation mixture (total volume of 100 µL) contains an NADPH-generating system (1 IU/mL glucose-6-phosphate dehydrogenase, 2 mM glucose-6-phosphate, 0.5 mM NADP⁺, 4 mM MgCl₂), 100 mM potassium phosphate buffer (pH 7.4), 0.1 mM EDTA, and 50 µM triazolam as a substrate. The incubation times (30 minutes) and protein concentrations of microsomes (0.1 mg/mL) used were selected from the linear range of formation of triazolam metabolites. Reactions were started by the addition of the NADPH-generation system (10 µL) after preincubation of the mixtures for 1 minute at 37°C. To stop incubation, 500 µL of acetonitrile/methanol/formic acid [500/500/1 (v/v/v)] was added. As an internal control, 10 µL of 0.25 µg/mL propranolol in methanol was added to the supernatant (100 µL). Determination of 1'-hydroxytriazolam and 4-hydroxytriazolam was carried out using liquid chromatography-tandem mass spectrometry (LC-MS/MS).

Pharmacokinetic Analysis of Triazolam. WT, 2c3aKO, and hCYP3A/2c3aKO mice (*n* = 4 per group) were orally administered with triazolam (1 mg/kg). Blood samples were collected from suborbital veins using a heparinized capillary tube at 15, 30, 45, 60, and 120 minutes after triazolam dosing. Plasma was separated and kept at -80°C until determination. Plasma (10 µL) was mixed with 50 µL of propranolol (0.05 µg/mL) as an internal standard. Propranolol solution was prepared in acetonitrile containing 0.1% (v/v) formic acid. Mixed samples were centrifuged at 15,000g for 10 minutes, and then 45 µL of the supernatant was mixed with 75 µL of a mixture consisting of 0.1% (v/v) formic acid in methanol and distilled water (3/2, v/v). The filtrate was subjected to determine the concentrations of triazolam, 1'-hydroxytriazolam and 4-hydroxytriazolam by LC-MS/MS. AUC from 0 to 120 minutes was calculated using the linear trapezoidal method.

Pharmacokinetic Analysis of Clobazam. hCYP3A/3aKO and hCYP3A/2c3aKO mice (*n* = 4 per group) were orally administered with CLB (10 mg/kg). At 0.25, 0.5, 1, 2, 4, and 24 hours after CLB dosing; blood samples were collected as described above. At an interval of 2 weeks, the mice were orally treated with phenobarbital (100 mg/kg per day) for 3 days. After 18 hours of final dosing, the mice were orally treated with CLB (10 mg/kg). Blood samples were collected as described above, and plasma was kept at -80°C. Plasma (10 µL) was mixed with 80 µL of oxazepam (0.018 µg/mL in methanol) as an internal standard. After centrifugation at 15,000g for 10 minutes, 75 µL of the supernatant

and 25 μ L of distilled water were mixed and filtered. The sample was subjected to determine the concentrations of CLB and NCLB by LC-MS/MS. AUC from 0 to 24 hours was calculated using the linear trapezoidal method.

Determination of TRZ, CLB, and Their Metabolites. Quantification of triazolam, CLB, and their metabolites in plasma and incubation mixture was performed by LC-MS/MS analysis. The conditions are shown in Supplemental Table 3.

Statistical Analysis. Data are expressed as means with S.D. Statistical analyses were performed by using Statcel (OMS, Tokyo, Japan). Comparisons of multiple groups were performed by one-way ANOVA with a post hoc test of Scheffé's

F test. Comparison of two groups was made with Welch's *t* test or paired samples *t* test. *P* < 0.05 was considered statistically significant.

Results

mRNA Expression. hCYP3A/2c3aKO mice were generated by crossing hCYP3A/3aKO and Cyp2cKO mice. Genomic PCR confirmed the genotype of hCYP3A/2c3aKO, and FISH analysis showed that the MAC carrying the human *CYP3A* gene cluster (hCYP3A-MAC) was stably maintained without integration into the host genome in hCYP3A/2c3aKO mice (Supplemental Fig. 2). To confirm that the expression of

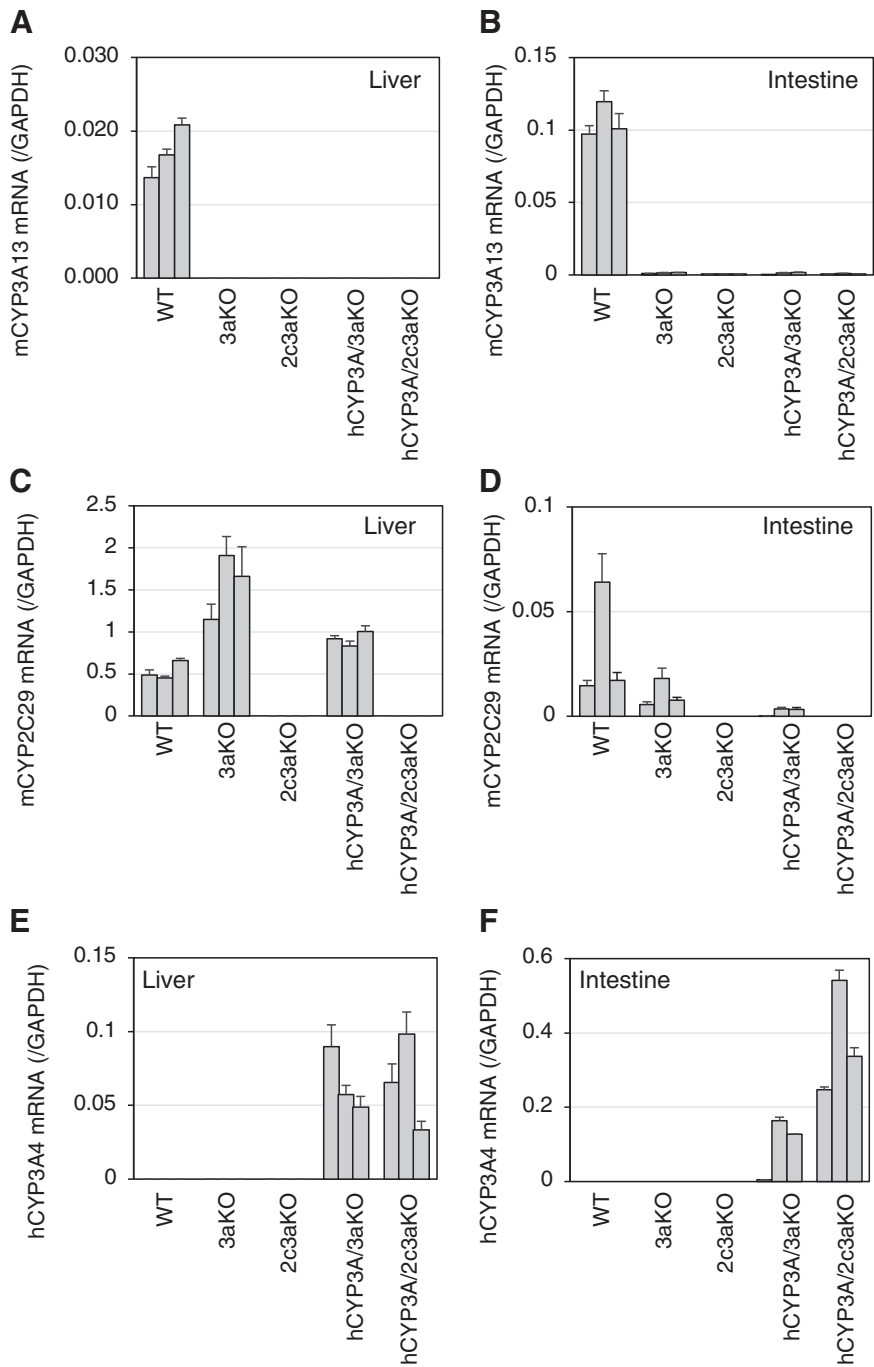


Fig. 1. Expression levels of mCYP3A13 (A and B), mCYP2C29 (C and D), and hCYP3A4 (E and F) mRNAs in the liver (A, C, and E) and intestine (B, D, and F) of WT, 3aKO, 2c3aKO, hCYP3A/3aKO, and hCYP3A/2c3aKO mice. The mRNA expression levels were normalized by expression levels of GAPDH mRNA. Data for each mouse (n = 3 per group) are shown as means with S.D. of three independent determinations, each performed in duplicate.

mouse endogenous *Cyp2c* and *Cyp3a* genes was lost, quantitative PCR analyses for CYP3A13 and CYP2C29, which are expressed in the liver and small intestine of WT mice (Martignoni et al., 2006; Graves et al., 2017), were performed. As shown in Fig. 1, A and B, the expression of mouse CYP3A13 mRNA was found in the liver and small intestine of WT mice. On the other hand, the expression of CYP3A13 was negligible in other mouse lines. As shown in Fig. 2, A and B, the expression of mouse CYP2C29 mRNA was found in the liver and small intestine of WT, 3aKO, and hCYP3A/3aKO mice but not in those of 2c3aKO and hCYP3A/2c3aKO mice. Consistent with previous results (Mingishi et al., 2019), the expression levels of CYP2C29 mRNA in the livers of 3aKO and hCYP3A/3aKO mice were higher than those in the livers of WT mice. These findings confirmed that mouse endogenous *Cyp2c* and *Cyp3a* genes were deleted in 2c3aKO and hCYP3A/2c3aKO mice.

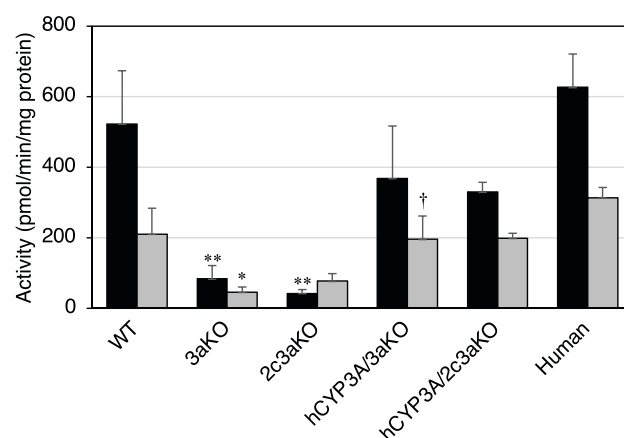
Next, we checked the expression of the human CYP3A4 mRNA in the liver and small intestine. As shown in Fig. 1, E and F, the expression of CYP3A4 mRNA was found in the liver and small intestine of hCYP3A/2c3aKO mice as well as hCYP3A/3aKO mice. In one hCYP3A/3aKO mouse, the expression level of intestinal CYP3A4 mRNA was low, but the expression levels of hepatic CYP3A4 mRNA were similar in hCYP3A/3aKO and hCYP3A/2c3aKO mice. Since the mRNA expression levels of GAPDH were also similar to those in other mice (data not shown), the possibility of a sampling error or mRNA degradation was excluded.

To examine the compensatory effects of double KO of *Cyp2c* and *Cyp3a* genes, we determined the mRNA expression levels of mouse CYP1A2 in the liver and CYP2B10, UGT1A1, and Mdr1a in the liver and intestine of WT, 3aKO, 2c3aKO, hCYP3A/3aKO, and hCYP3A/2c3aKO mice. As shown in Supplemental Table 4, the expression levels of CYP2B10 mRNA in the liver of 2c3aKO mice were significantly higher than those of WT and 3aKO mice. The expression levels of CYP2B10 mRNA in the liver of hCYP3A/2c3aKO mice were lower than those of 2c3aKO mice. The 2c3aKO mice also expressed higher mRNA levels of UGT1A1 and Mdr1a compared with WT mice. For intestines, there were no significant differences in the mRNA expression levels between the five mouse lines examined.

Enzyme Activity in the Liver and Intestine. Since CYP3A4 protein was detected in the microsomes from liver and intestine of hCYP3A/3aKO and hCYP3A/2c3aKO mice (Supplemental Fig. 3), we investigated the functional expression of human CYP3A4 in hCYP3A/3aKO and hCYP3A/2c3aKO mice. The metabolites of triazolam formed by CYP3A, 1'-hydroxytriazolam, and 4-hydroxytriazolam were determined as markers of CYP3A activities (Kazuki et al., 2013). As shown in Fig. 2, A and B, 1'-hydroxytriazolam and 4-hydroxytriazolam were formed in the microsomes prepared from liver and intestine of WT, hCYP3A/3aKO, and hCYP3A/2c3aKO mice and humans. The formation rates of 1'-hydroxytriazolam and 4-hydroxytriazolam in the liver microsomes of 3aKO and 2c3aKO mice were lower than those in the liver microsomes of WT, hCYP3A/3aKO, and hCYP3A/2c3aKO mice, although the metabolites were detected. On the other hand, the formation of these metabolites in the intestine microsomes was negligible in 3aKO and 2c3aKO mice.

Furthermore, the effect of ketoconazole, a CYP3A inhibitor, on the formation of 1'-hydroxytriazolam and 4-hydroxytriazolam in the liver microsomes was examined for WT, 2c3aKO, and hCYP3A/2c3aKO mice and humans. As shown in Fig. 3, the formation rates of metabolites in the liver microsomes of WT and hCYP3A/2c3aKO mice and humans were decreased by ketoconazole, whereas no effect was found in the liver microsomes of 2c3aKO mice. Although the inhibitory effect of ketoconazole was potent in WT mice, they were similar between hCYP3A/2c3aKO mice and humans.

A Liver



B Intestine

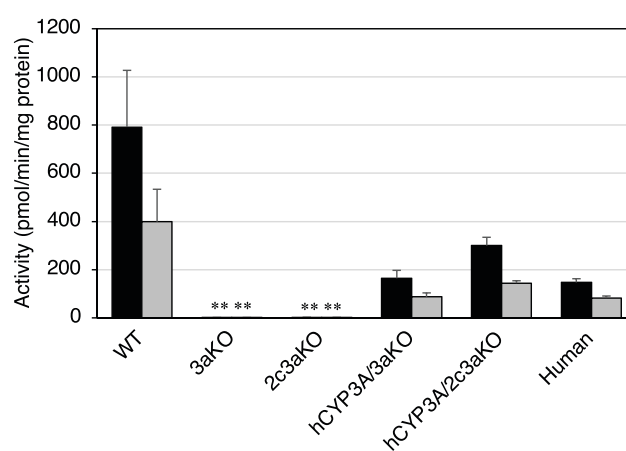


Fig. 2. Metabolic activity of a CYP3A probe substrate, triazolam, in the liver (A) and intestine (B) microsomes of mice and humans. Formation rates of 1'-hydroxytriazolam (black bar) and 4-hydroxytriazolam (gray bar) from triazolam (50 μ M) were determined by using liver and intestine microsomes. Data are expressed as means with S.D. ($n = 3$ per group) of three independent experiments, each performed in duplicate. *** $P < 0.01$ compared with WT; † $P < 0.05$ compared with 3aKO (one-way ANOVA with a post hoc test of Scheffé's F test).

Pharmacokinetics of Triazolam and Its Metabolites. Plasma concentration-time profiles of triazolam and its metabolites after oral dosing of triazolam and their AUC values are shown in Fig. 4 and Table 1, respectively. In WT mice, plasma levels and AUC values of 1'-hydroxytriazolam were higher than those of triazolam and 4-hydroxytriazolam. On the other hand, plasma levels of 1'-hydroxytriazolam in 2c3aKO mice were much lower than those of triazolam and 4-hydroxytriazolam. AUC values of 1'-hydroxytriazolam in 2c3aKO mice were more than 30-fold lower than those in WT mice. In addition, AUC ratios of 1'-hydroxytriazolam/triazolam in 2c3aKO mice were much lower than those in WT mice, although AUC ratios of 4-hydroxytriazolam/triazolam were not different between WT and 2c3aKO mice (Table 2). These results indicated that formation of 1'-hydroxytriazolam was selectively decreased in 2c3aKO mice. In hCYP3A/2c3aKO mice, AUC values of 1'-hydroxytriazolam were about sixfold higher than those in 2c3aKO mice, although the levels of 4-hydroxytriazolam were lower than those in 2c3aKO mice. The AUC ratios of 1'-hydroxytriazolam/triazolam in hCYP3A/2c3aKO mice were about eightfold higher than those in 2c3aKO mice. The AUC ratios of 4-hydroxytriazolam/triazolam were not different between

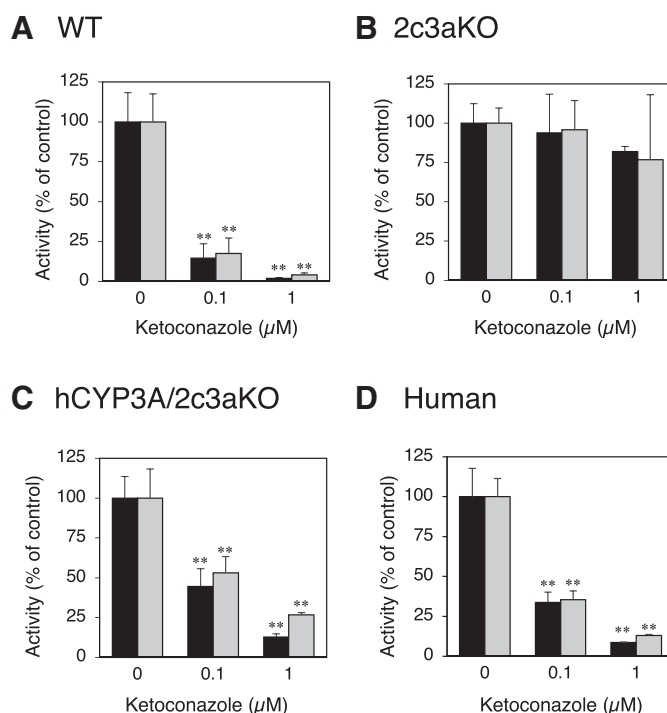


Fig. 3. Effect of ketoconazole on metabolic activity of triazolam in the liver microsomes of WT (A), 2c3aKO (B), and hCYP3A/2c3aKO (C) mice and humans (D). Triazolam (50 μ M) was incubated with pooled microsomes ($n = 3$ per group) in the presence or absence of ketoconazole (0.1 and 1 μ M). Activities of 1'-hydroxylation (black bar) and 4-hydroxylation (gray bar) were shown as % of control (0 μ M ketoconazole). Data are expressed as means with S.D. of three independent experiments, each performed in duplicate. *** $P < 0.01$ compared with control (one-way ANOVA with a post hoc test of Scheffé's F test).

hCYP3A/2c3aKO and 2c3aKO mice. These results show that preferential formation of 1'-hydroxytriazolam found in WT mice was diminished in 2c3aKO mice and that the formation of 1'-hydroxytriazolam was increased by the introduction of the human *CYP3A* gene cluster. On the other hand, no different AUC ratios of 1'-hydroxytriazolam/triazolam and 4-hydroxytriazolam/triazolam were found between hCYP3A/3aKO and 3aKO mice, although AUC ratios of 4-hydroxytriazolam/triazolam in hCYP3A/3aKO mice showed a tendency to be higher than those in 3aKO mice (Supplemental Fig. 4; Supplemental Table 1).

CLB Metabolism in Vivo. To investigate the roles of CYP3A and CYP2C in the sequential metabolism of CLB, plasma concentration-time profiles of CLB and NCLB were assessed in hCYP3A/3aKO and hCYP3A/2c3aKO mice (Fig. 5, A and B). Plasma levels of CLB were much lower than those of NCLB in both mouse lines, suggesting extensive metabolism of CLB to NCLB. hCYP3A/2c3aKO mice showed a higher mean AUC of CLB (Table 3) and slower elimination of NCLB than those in hCYP3A/3aKO mice. Next, the effect of a CYP3A inducer, phenobarbital, on the CLB disposition was examined. In hCYP3A/3aKO mice, plasma levels and AUC values of CLB and NCLB were decreased by phenobarbital treatment (Fig. 5, A and C; Table 3). For CLB, decreases of plasma levels and AUC values were also found in hCYP3A/2c3aKO mice treated with phenobarbital (Fig. 5, B and D; Table 3). On the other hand, the effect of phenobarbital on the plasma levels of NCLB was small in hCYP3A/2c3aKO mice. Elimination of NCLB in hCYP3A/2c3aKO mice was slower than that in hCYP3A/3aKO mice with or without phenobarbital treatment. In this study, two hCYP3A/2c3aKO mice pretreated with phenobarbital died after dosing of CLB, unlike hCYP3A/3aKO mice. Since plasma concentrations of phenobarbital in the hCYP3A/2c3aKO mice that survived were more than 10-fold higher than those in hCYP3A/

3aKO mice (data not shown), adverse effects such as excessive sedation may be evoked by phenobarbital at a dose of 100 mg/kg.

Discussion

In our *in vitro* and *in vivo* studies, we showed that the formation of 1'-hydroxytriazolam was markedly decreased in 2c3aKO mice compared with that in 3aKO mice. Previous *in vitro* studies also showed that the metabolism of triazolam (1'-hydroxylation and 4-hydroxylation) was reduced in 3aKO mice (van Waterschoot et al., 2009; Kazuki et al., 2013, 2019; Minegishi et al., 2019). However, formation of 1'-hydroxytriazolam was not completely diminished in the liver microsomes of 3aKO mice (van Waterschoot et al., 2009; Minegishi et al., 2019). In addition, plasma levels of 1'-hydroxytriazolam in 3aKO mice after oral administration of triazolam were not negligible (van Waterschoot et al., 2009). These findings clearly indicated that not only CYP3A but also other enzymes catalyzed the formation of 1'-hydroxytriazolam in 3aKO mice. Our previous *in vitro* study showed that an anti-CYP2C antibody inhibited the formation of 1'-hydroxytriazolam in the liver microsomes of 3aKO mice, suggesting that mouse endogenous CYP2C enzymes are responsible for the reaction (Minegishi et al., 2019). The results of the present study using liver microsomes indicated that the formation rate of 1'-hydroxytriazolam in 2c3aKO mice was lower than that in 3aKO mice, although the difference was not statistically significant (Fig. 2). Moreover, the AUC ratio of 1'-hydroxytriazolam/triazolam in 2c3aKO mice after oral dosing of triazolam was lower than that in 3aKO mice (Supplemental Fig. 4). These results suggest that double KO of mouse *Cyp2c* and *Cyp3a* genes is effective for reducing the formation of 1'-hydroxytriazolam from triazolam in mice.

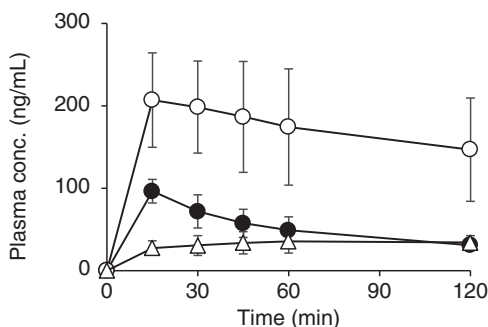
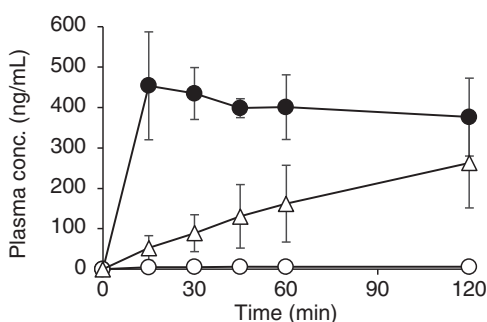
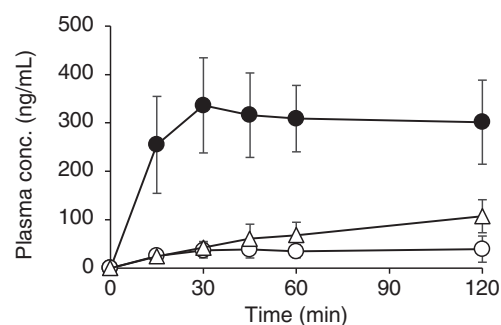
A WT**B 2c3aKO****C hCYP3A/2c3aKO**

Fig. 4. Plasma concentrations of triazolam, 1'-hydroxytriazolam, and 4-hydroxytriazolam in WT (A), 2c3aKO (B), and hCYP3A/2c3aKO (C) mice. Mice ($n = 4$ per group) were given an oral dose of triazolam (1 mg/kg). Plasma concentrations of triazolam (closed circles), 1'-hydroxytriazolam (open circles), and 4-hydroxytriazolam (open triangles) were determined. Each point represents the mean with S.D.

Generation of hCYP3A mice with a background of double KO for *Cyp2c* and *Cyp3a* genes succeeded in showing a gain of function for human CYP3A-mediated 1'-hydroxylation of triazolam *in vitro* and *in vivo*. Plasma levels of 1'-hydroxytriazolam in hCYP3A/2c3aKO

mice after oral dosing of triazolam were higher than those in 2c3aKO mice (Fig. 4). Notably, it was shown that the AUC ratio of 1'-hydroxytriazolam/triazolam reflected the function of human CYP3A enzymes (Table 2; Supplemental Fig. 4). Therefore, we suggest that the AUC ratio of 1'-hydroxytriazolam/triazolam after oral dosing of triazolam reflects the function of human CYP3A in hCYP3A/2c3aKO mice.

We previously reported that 4-hydroxytriazolam was a possible marker of CYP3A functions in mice after intravenous dosing of triazolam (Minegishi et al., 2019). This finding was supported by a drug-drug interaction study using hCYP3A/3aKO mice (Minegishi et al., 2021). In the present study, the AUC ratio of 4-hydroxytriazolam/triazolam in hCYP3A/3aKO mice was higher than that in 3aKO mice after oral administration of triazolam (Supplemental Table 1), suggesting that the formation of 4-hydroxytriazolam reflected human CYP3A functions in hCYP3A/3aKO mice after oral dosing of triazolam. On the other hand, higher plasma levels of 4-hydroxytriazolam were found in 2c3a-KO mice than those in WT mice (Fig. 4). The AUC of 4-hydroxytriazolam in 2c3a-KO mice was about fivefold higher than that in WT mice (Table 1). Since the formation of 1'-hydroxytriazolam was almost completely reduced in 2c3a-KO mice, the formation of 4-hydroxytriazolam might proceed as a complementary reaction. In addition, there is a possibility that mouse CYP2C and CYP3A enzymes are involved in the elimination of 4-hydroxytriazolam such as transformation to 1',4-dihydroxytriazolam. Namely, 4-hydroxytriazolam is not suitable as a probe of CYP3A functions in hCYP3A/2c3aKO mice, unlike hCYP3A/3aKO mice.

In humans, CLB, an antiepileptic drug, is mainly metabolized to its active metabolite NCLB by CYP3A (Giraud et al., 2004). Several reports indicated that phenobarbital decreased plasma levels of CLB and increased the NCLB/CLB ratio in patients with epilepsy (Bun et al., 1986; Sennoune et al., 1992; Theis et al., 1997). The findings implied that phenobarbital may stimulate the metabolism of CLB to NCLB. The present study showed that AUC values of CLB in hCYP3A/3aKO mice were more than 10-fold decreased by phenobarbital (Table 3). A marked decrease in AUC values of CLB was found in hCYP3A/2c3aKO mice. In addition, the AUC ratio of NCLB/CLB in hCYP3A/3aKO and hCYP3A/2c3aKO mice was increased by phenobarbital. These results indicated that phenobarbital enhanced the metabolism of CLB to NCLB in both hCYP3A/3aKO and hCYP3A/2c3aKO mice, in agreement with the findings in humans. Phenobarbital activates the nuclear receptor constitutive androstane receptor in the livers of both humans and mice, resulting in induction of the expression of CYP3A enzymes (Kobayashi et al., 2015). Therefore, enhanced metabolism of CLB to NCLB in hCYP3A/3aKO and hCYP3A/2c3aKO mice was thought to be mediated *via* induction of human CYP3A by phenobarbital.

The conversion of CLB to NCLB is also catalyzed by CYP2C19 and CYP2B6 (Giraud et al., 2004). CYP2C19 also catalyzes the conversion of CLB to 4'-hydroxy CLB, a minor metabolic pathway. The results of the present study showed that the mean AUC value of CLB in hCYP3A/2c3aKO mice was 13-fold higher than that in hCYP3A/3aKO mice (Table 3), suggesting that mouse endogenous CYP2C enzymes are involved in the elimination of CLB. It is still unclear whether mouse endogenous CYP2B enzymes catalyze the metabolism of CLB.

TABLE 1

AUC₀₋₁₂₀ values of triazolam and its metabolites in WT, 2c3aKO, and hCYP3A/2c3aKO mice

Data are expressed as means \pm S.D. ($n = 4$ per group). * $P < 0.05$; ** $P < 0.01$ compared with WT (one-way ANOVA with a post hoc test of Scheffé's F test).

Compounds	WT	2c3aKO	hCYP3A/2c3aKO
Triazolam ($\mu\text{g}\cdot\text{min/mL}$)	6.15 \pm 1.43	45.6 \pm 8.3**	34.2 \pm 7.5**
1'-Hydroxytriazolam ($\mu\text{g}\cdot\text{min/mL}$)	19.8 \pm 6.44	0.625 \pm 0.168**	3.99 \pm 1.86**
4-Hydroxytriazolam ($\mu\text{g}\cdot\text{min/mL}$)	3.74 \pm 1.22	18.0 \pm 9.2*	7.67 \pm 3.23

AUC₀₋₁₂₀, AUC from 0 to 120 minutes.

TABLE 2

AUC ratios of triazolam and its metabolites in WT, 2c3aKO, and hCYP3A/2c3aKO mice
Data are expressed as means ± S.D. (n = 4 per group). *P < 0.05; **P < 0.01 compared with WT (one-way ANOVA with a post hoc test of Scheffé's F test).

Metabolite/Triazolam	WT	2c3aKO	hCYP3A/2c3aKO
1'-Hydroxytriazolam/triazolam	3.19 ± 0.35	0.0137 ± 0.0021**	0.113 ± 0.032**
4-Hydroxytriazolam/triazolam	0.600 ± 0.070	0.407 ± 0.238	0.222 ± 0.064*

NCLB is further metabolized to 4'-hydroxy NCLB by CYP2C19 (Giraud et al., 2004). Since CYP2C19 is a genetically polymorphic enzyme, it is speculated that poor metabolizers of CYP2C19 show prolonged NCLB elimination. However, there is no report on a detailed pharmacokinetic study. In clinical studies, steady-state concentrations of CLB and NCLB in the plasma of patients were determined, and it was shown that NCLB concentrations and NCLB/CLB ratios in poor

metabolizers of CYP2C19 were higher than those in extensive metabolizers who carried no mutated allele of the *CYP2C19* gene (Contin et al., 2002; Kosaki et al., 2004; Seo et al., 2008; Saruwatari et al., 2014). In the present study, the mean AUC value of NCLB in hCYP3A/2c3aKO mice was threefold higher than that in hCYP3A/3aKO mice (Table 3). However, the AUC ratio of NCLB/CLB in hCYP3A/2c3aKO mice was lower than that in hCYP3A/3aKO mice.

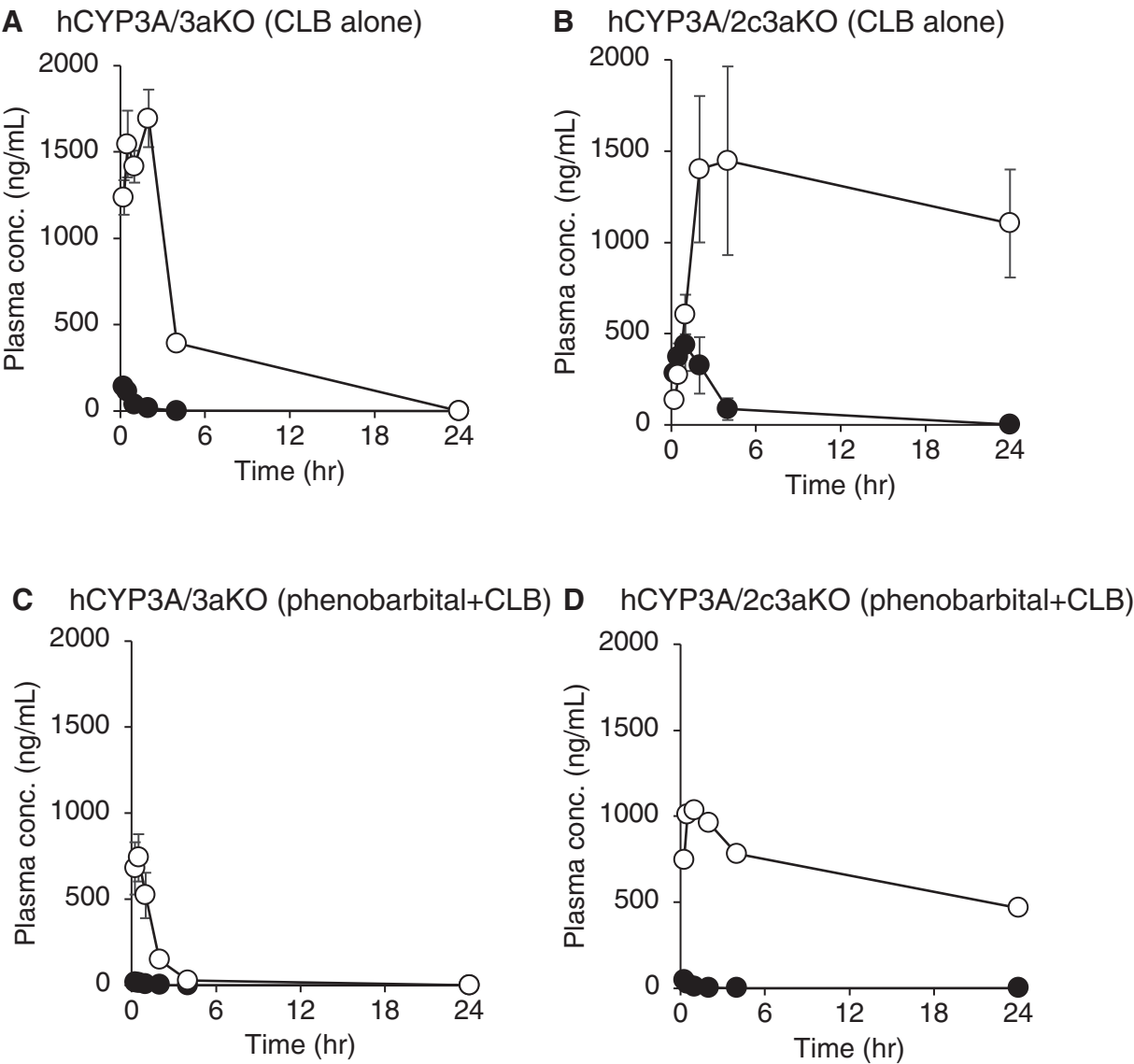


Fig. 5. Plasma concentrations of CLB and NCLB in hCYP3A/3aKO (A and C) and hCYP3A/2c3aKO (B and D) mice. Mice (n = 4 per group) were given an oral dose of CLB (10 mg/kg). After 2 weeks of washout, the mice were given an oral dose of phenobarbital (100 mg/kg) for three days followed by an oral dose of CLB (10 mg/kg). Plasma concentrations of CLB (closed circles) and NCLB (open circles) were determined. Each point represents the mean with S.D. Since two hCYP3A/2c3aKO mice pretreated with phenobarbital died after dosing of CLB, data for hCYP3A/2c3aKO mice that survived are shown as means.

TABLE 3

AUC₀₋₂₄ values of CLB and NCLB and AUC ratios (NCLB/CLB) in hCYP3A/3aKO and hCYP3A/2c3aKO mice

Data are shown as means \pm S.D. ($n = 4$ per group). Data for hCYP3A/2c3aKO mice treated with phenobarbital are individual values of two mice because two mice died. * $P < 0.05$ compared with hCYP3A/3aKO mice (Welch's t test); *** $P < 0.001$ compared with hCYP3A/3aKO mice (Student's t test); # $P < 0.05$, ## $P < 0.001$ compared with control (paired samples t test).

Compounds	CLB Alone		Phenobarbital + CLB	
	hCYP3A/3aKO	hCYP3A/2c3aKO	hCYP3A/3aKO	hCYP3A/2c3aKO
CLB ($\mu\text{g}\cdot\text{hr}/\text{mL}$)	0.151 \pm 0.028	1.977 \pm 0.997*	0.012 \pm 0.003##	0.062, 0.037
NCLB ($\mu\text{g}\cdot\text{hr}/\text{mL}$)	8.811 \pm 0.559	29.643 \pm 8.979*	1.347 \pm 0.067	19.380, 12.721
NCLB/CLB	59.5 \pm 7.97	16.4 \pm 3.92***	115.9 \pm 28.9 [#]	311.06, 341.04

AUC₀₋₂₄, AUC from 0 to 24 hours.

Since plasma elimination of NCLB in hCYP3A/2c3aKO mice was markedly prolonged compared with that in hCYP3A/3aKO mice (Fig. 5, A and B), the NCLB/CLB ratio in plasma in a steady state after repeated administration of CLB would be increased in hCYP3A/2c3aKO mice. Even after pretreatment with phenobarbital, plasma elimination of NCLB in hCYP3A/2c3aKO mice was markedly prolonged compared with that in hCYP3A/3aKO mice (Fig. 5, C and D). This result suggests that NCLB concentrations and NCLB/CLB ratios in a steady state are high in poor metabolizers of CYP2C19 who are coadministered phenobarbital.

Genetically humanized mice for drug-metabolizing enzymes have been considered to be useful models that can improve the predictive accuracy of pharmacokinetics and toxicity in humans. The advantages are that 1) transplantation in each experiment is not needed, unlike chimera mice with human hepatocytes; 2) genetic background is controlled; and 3) human genes are expressed in targeted organs. On the other hand, the disadvantages are that 1) genetic factors other than the loaded genes originate from mice and 2) knockout of genes often leads to compensatory effects.

In conclusion, the formation of 1'-hydroxytriazolam was dramatically decreased in 2c3aKO mice. Metabolic functions of human CYP3A enzymes were distinctly found in hCYP3A mice with the background of 2c3aKO. Pharmacokinetic studies with hCYP3A/2c3aKO mice and hCYP3A/3aKO mice would be useful to study the polymorphic effects of CYP2C genes (e.g., CYP2C9 and CYP2C19) on *in vivo* profiles of drugs metabolized by CYP2C and CYP3A. The novel hCYP3A mice without mouse *Cyp2c* and *Cyp3a* genes are expected to be a useful to evaluate human CYP3A-mediated metabolism *in vivo*.

Acknowledgments

We thank Toko Kurosaki, Yukako Sumida, Masami Morimura, Kei Yoshida, Eri Kaneda, Michika Fukino, Asahi Shibahara, and Tomoko Ashiba at Tottori University and Shoko Takehara, Kayoko Morimoto, and Haruka Takayama for their technical assistance. We also thank Dr. Hiroyuki Kugoh, Dr. Masaharu Hiratsuka, Dr. Tetsuya Ohbayashi, Dr. Hiroyuki Satofuka, and Dr. Takahito Ohira at Tottori University for critical discussions. This research was partly performed at the Tottori Bio Frontier managed by Tottori Prefecture.

Authorship Contributions

Participated in research design: Kobayashi, Y. Kazuki.

Conducted experiments: Kobayashi, Minegishi, Kuriyama, Abe, K. Kazuki.

Contributed new reagents or analytic tools: Abe, Y. Kazuki.

Performed data analysis: Kobayashi, Minegishi, Kuriyama, Miyajima, Abe, K. Kazuki.

Wrote or contributed to the writing of the manuscript: Kobayashi, Minegishi, Y. Kazuki.

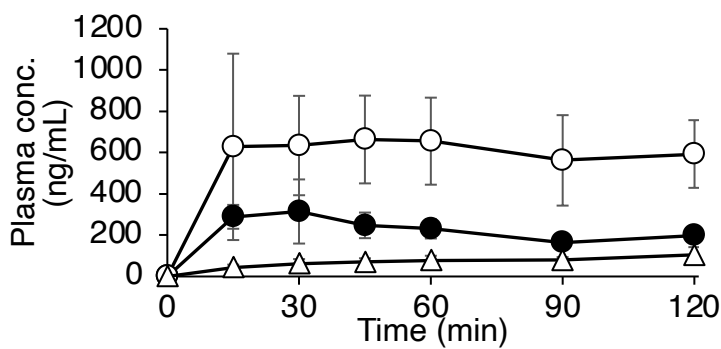
References

- Abe S, Kobayashi K, Oji A, Sakuma T, Kazuki K, Takehara S, Nakamura K, Okada A, Tsukazaki Y, Senda N, et al. (2017) Modification of single-nucleotide polymorphism in a fully humanized CYP3A mouse by genome editing technology. *Sci Rep* 7:15189.
- Bissig KD, Han W, Barzi M, Kovalchuk N, Ding L, Fan X, Pankowicz FP, Zhang QY, and Ding X (2018) P450-humanized and human liver chimeric mouse models for studying xenobiotic metabolism and toxicity. *Drug Metab Dispos* 46:1734–1744.
- Bun H, Coassolo P, Gouezo F, Serradimigni A, and Cano JP (1986) Time-dependence of clobazam and N-demethylclobazam kinetics in healthy volunteers. *Int J Clin Pharmacol Ther Toxicol* 24:287–293.
- Contin M, Sangiorgi S, Riva R, Parmeggiani A, Albani F, and Baruzzi A (2002) Evidence of polymorphic CYP2C19 involvement in the human metabolism of N-desmethyloclobazam. *Ther Drug Monit* 24:737–741.
- Giraud C, Tran A, Rey E, Vincent J, Tréluyer JM, and Pons G (2004) In vitro characterization of clobazam metabolism by recombinant cytochrome P450 enzymes: importance of CYP2C19. *Drug Metab Dispos* 32:1279–1286.
- Gonzalez FJ, Fang ZZ, and Ma X (2015) Transgenic mice and metabolomics for study of hepatic xenobiotic metabolism and toxicity. *Expert Opin Drug Metab Toxicol* 11:869–881.
- Graves JP, Gruzdev A, Bradbury JA, DeGraff LM, Edin ML, and Zeldin DC (2017) Characterization of the Tissue Distribution of the Mouse *Cyp2c* Subfamily by Quantitative PCR Analysis. *Drug Metab Dispos* 45:807–816.
- Hashimoto M, Kobayashi K, Watanabe M, Kazuki Y, Takehara S, Inaba A, Nitta SI, Senda N, Oshimura M, and Chiba K (2013) Knockout of mouse *Cyp3a* gene enhances synthesis of cholesterol and bile acid in the liver. *J Lipid Res* 54:2060–2068.
- Hashimoto M, Kobayashi K, Yamazaki M, Kazuki Y, Takehara S, Oshimura M, and Chiba K (2016) *Cyp3a* deficiency enhances androgen receptor activity and cholesterol synthesis in the mouse prostate. *J Steroid Biochem Mol Biol* 163:121–128.
- Kazuki Y, Kobayashi K, Aueviriyavit S, Oshima T, Kuroiwa Y, Tsukazaki Y, Senda N, Kawakami H, Ohtsuki S, Abe S, et al. (2013) Trans-chromosomal mice containing a human CYP3A cluster for prediction of xenobiotic metabolism in humans. *Hum Mol Genet* 22:578–592.
- Kazuki Y, Kobayashi K, Hirabayashi M, Abe S, Kajitani N, Kazuki K, Takehara S, Takiguchi M, Satoh D, Kuze J, et al. (2019) Humanized UGT2 and CYP3A transchromosomal rats for improved prediction of human drug metabolism. *Proc Natl Acad Sci USA* 116:3072–3081.
- Kobayashi K, Hashimoto M, Honkakoski P, and Negishi M (2015) Regulation of gene expression by CAR: an update. *Arch Toxicol* 89:1045–1055.
- Kobayashi K, Kuze J, Abe S, Takehara S, Minegishi G, Igarashi K, Kitajima S, Kanno J, Yamamoto T, Oshimura M, et al. (2019) CYP3A4 induction in the liver and intestine of pregnane X receptor/CYP3A-humanized mice: approaches by mass spectrometry imaging and portal blood analysis. *Mol Pharmacol* 96:600–608.
- Kosaki K, Tamura K, Sato R, Samejima H, Tanigawara Y, and Takahashi T (2004) A major influence of CYP2C19 genotype on the steady-state concentration of N-desmethyloclobazam. *Brain Dev* 26:530–534.
- Martignoni M, Groothuis G, and de Kanter R (2006) Comparison of mouse and rat cytochrome P450-mediated metabolism in liver and intestine. *Drug Metab Dispos* 34:1047–1054.
- Minegishi G, Kazuki Y, Nitta SI, Miyajima A, Akita H, and Kobayashi K (2021) *In vivo* evaluation of intestinal human CYP3A inhibition by macrolide antibiotics in CYP3A-humanised mice. *Xenobiotica* 51:764–770.
- Minegishi G, Kazuki Y, Yamasaki Y, Okuya F, Akita H, Oshimura M, and Kobayashi K (2019) Comparison of the hepatic metabolism of triazolam in wild-type and *Cyp3a*-knockout mice for understanding CYP3A-mediated metabolism in CYP3A-humanised mice *in vivo*. *Xenobiotica* 49:1303–1310.
- Satoh D, Abe S, Kobayashi K, Nakajima Y, Oshimura M, and Kazuki Y (2018) Human and mouse artificial chromosome technologies for studies of pharmacokinetics and toxicokinetics. *Drug Metab Pharmacokinet* 33:17–30.
- Saruwatari J, Ogusu N, Shimomasuda M, Nakashima H, Seo T, Tanikawa K, Tsuda Y, Nishimura M, Nagata R, Yasui-Furukori N, et al. (2014) Effects of CYP2C19 and P450 oxidoreductase polymorphisms on the population pharmacokinetics of clobazam and N-desmethyloclobazam in Japanese patients with epilepsy. *Ther Drug Monit* 36:302–309.
- Scheer N, Kapelyukh Y, Chatham L, Rode A, Buechel S, and Wolf CR (2012) Generation and characterization of novel cytochrome P450 *Cyp2c* gene cluster knockout and CYP2C9 humanized mouse lines. *Mol Pharmacol* 82:1022–1029.
- Sennoune S, Mesdjan E, Bonneton J, Genton P, Dravet C, and Roger J (1992) Interactions between clobazam and standard antiepileptic drugs in patients with epilepsy. *Ther Drug Monit* 14:269–274.
- Seo T, Nagata R, Ishitsu T, Murata T, Takaishi C, Hori M, and Nakagawa K (2008) Impact of CYP2C19 polymorphisms on the efficacy of clobazam therapy. *Pharmacogenomics* 9:527–537.
- Theis JG, Koren G, Daneman R, Sherwin AL, Menzano E, Cortez M, and Hwang P (1997) Interactions of clobazam with conventional antiepileptics in children. *J Child Neurol* 12:208–213.

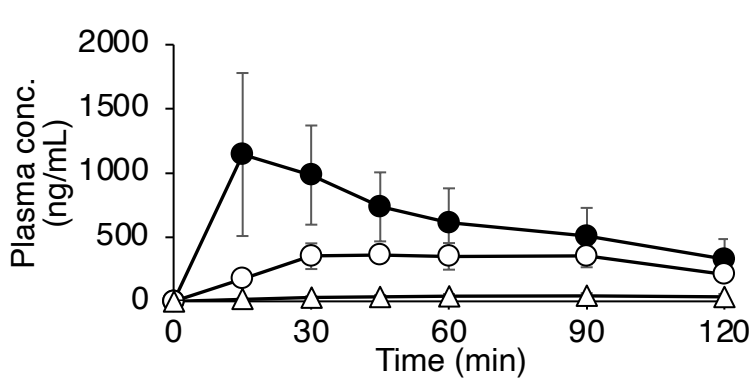
- Tomizuka K, Yoshida H, Uejima H, Kugoh H, Sato K, Ohguma A, Hayasaka M, Hanaoka K, Oshimura M, and Ishida I (1997) Functional expression and germline transmission of a human chromosome fragment in chimaeric mice. *Nat Genet* **16**:133–143.
- van Waterschoot RA, Rooswinkel RW, Sparidans RW, van Herwaarden AE, Beijnen JH, and Schinkel AH (2009) Inhibition and stimulation of intestinal and hepatic CYP3A activity: studies in humanized CYP3A4 transgenic mice using triazolam. *Drug Metab Dispos* **37**:2305–2313.
- van Waterschoot RA, van Herwaarden AE, Lagas JS, Sparidans RW, Wagenaar E, van der Kruijsen CM, Goldstein JA, Zeldin DC, Beijnen JH, and Schinkel AH (2008) Midazolam metabolism in cytochrome P450 3A knockout mice can be attributed to up-regulated CYP2C enzymes. *Mol Pharmacol* **73**:1029–1036.
- Zanger UM and Schwab M (2013) Cytochrome P450 enzymes in drug metabolism: regulation of gene expression, enzyme activities, and impact of genetic variation. *Pharmacol Ther* **138**:103–141.

Address correspondence to: Dr. Kaoru Kobayashi, Department of Biopharmaceutics, Graduate School of Clinical Pharmacy, Meiji Pharmaceutical University, 2-522-1 Noshio, Kiyose, Tokyo 204-8588, Japan. E-mail: kaoruk@my-pharm.ac.jp; or Dr. Yasuhiro Kazuki, Department of Chromosome Biomedical Engineering School of Life Science, Faculty of Medicine, Tottori University, 86 Nishi-cho, Yonago, Tottori 683-8503, Japan. E-mail: kazuki@tottori-u.ac.jp

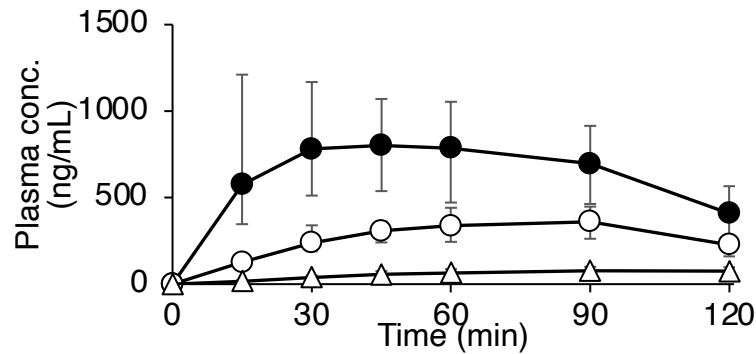
A. WT



B. 3aKO



C. hCYP3A/3aKO



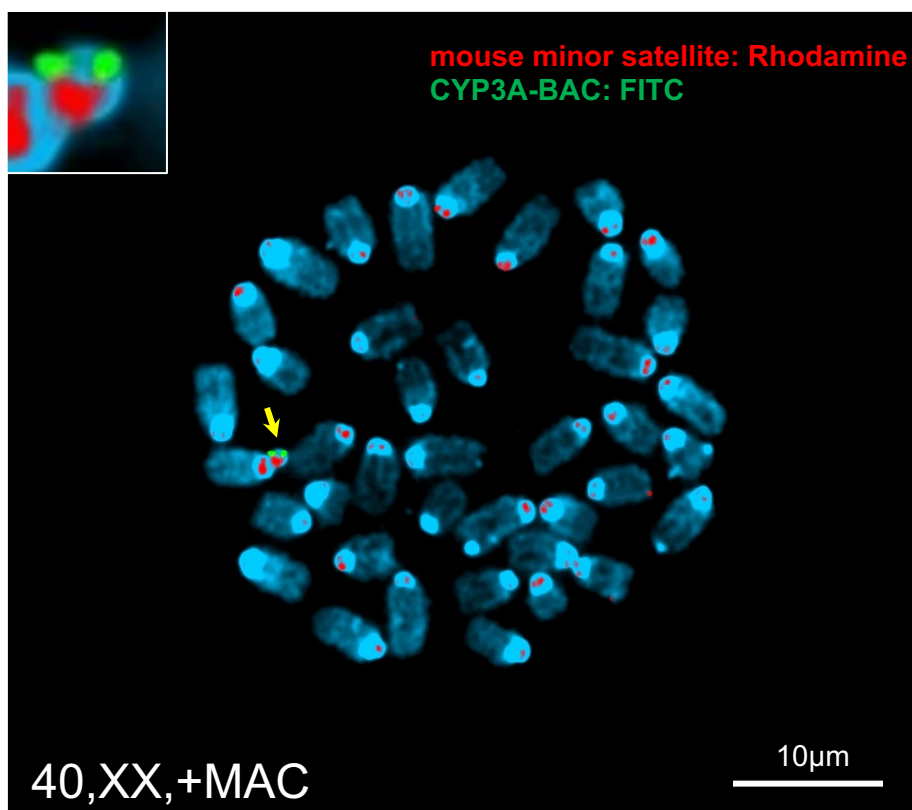
Supplemental Fig. 1 Plasma concentrations of triazolam, 1'-hydroxytriazolam and 4-hydroxytriazolam in WT (A), 3aKO (B) and hCYP3A/3aKO (C) mice.
Mice (n = 5/group) were given an oral dose of triazolam (2 mg/kg). Plasma concentrations of triazolam (closed circles), 1'-hydroxytriazolam (open circles) and 4-hydroxytriazolam (open triangles) were determined. Each point represents the mean with S. D.

Metabolic disposition of triazolam and clobazam in humanized CYP3A mice with a double knockout background of mouse *Cyp2c* and *Cyp3a* genes

Kaoru Kobayashi, Genki Minegishi, Nina Kuriyama, Atsushi Miyajima, Satoshi Abe, Kanako Kazuki, Yasuhiro Kazuki

Drug Metabolism and Disposition

Manuscript Number: DMD-AR-2022-001087



Supplemental Fig. 2 Retention of CYP3A-MAC in hCYP3A/2c3aKO mice.

Representative FISH image of metaphase spreads from lymphocytes in hCYP3A/2c3aKO mice. Yellow arrow indicates CYP3A-MAC which is enlarged as inset.

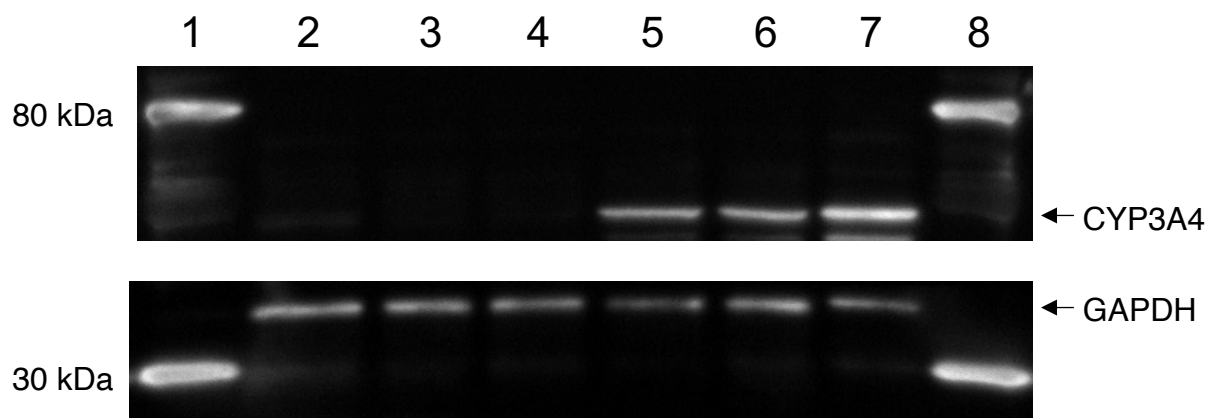
Metabolic disposition of triazolam and clobazam in humanized CYP3A mice with a double knockout background of mouse *Cyp2c* and *Cyp3a* genes

Kaoru Kobayashi, Genki Minegishi, Nina Kuriyama, Atsushi Miyajima, Satoshi Abe, Kanako Kazuki, Yasuhiro Kazuki

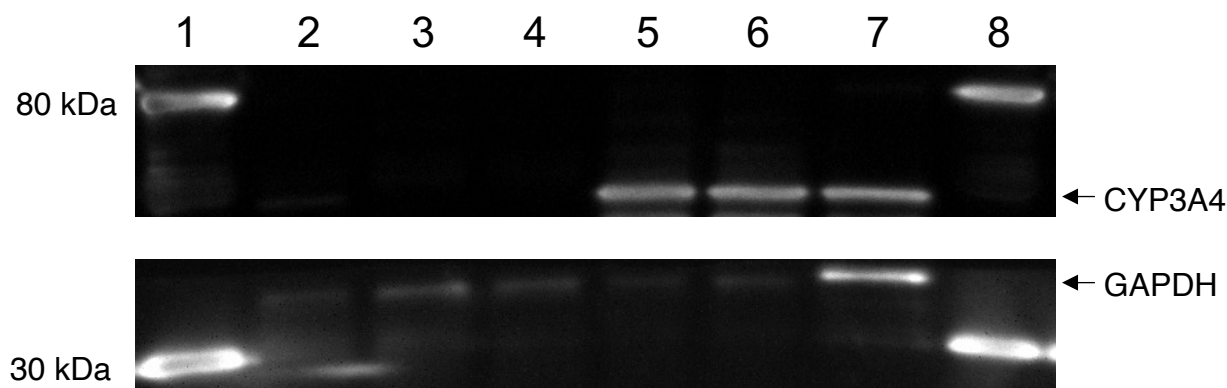
Drug Metabolism and Disposition

Manuscript Number: DMD-AR-2022-001087

A. Liver

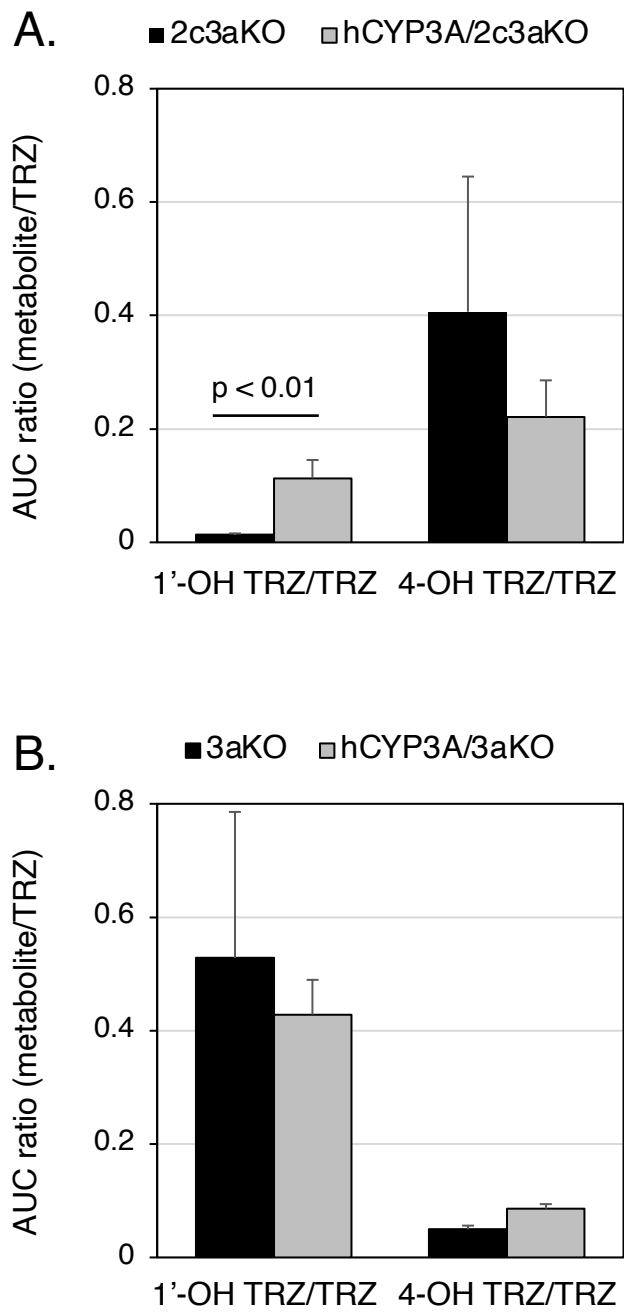


B. Intestine



Supplemental Fig. 3 Expression CYP3A protein in the liver and intestine of hCYP3A/3aKO and hCYP3A/2c3aKO mice.

Microsomal proteins (4 µg/lane) of livers and small intestines were applied to gels. Lane 1: ladder, lane 2: WT, lane 3: 3aKO, lane 4: 2c3aKO, lane 5: hCYP3A/3aKO, lane 6: hCYP3A/2c3aKO, lane 7: human, lane 8: ladder. A mouse monoclonal anti-CYP3A4 antibody (1:2000, sc-53850) and a rabbit monoclonal anti-GAPDH antibody (1:10000, ab181602) were used as Primary antibodies.



Supplemental Fig. 4 AUC ratios (metabolite/TRZ) in 2c3aKO, hCYP3A/2c3aKO, 3aKO and hCYP3A/3aKO mice.
(A) AUC ratios in 2c3aKO and hCYP3A/2c3aKO mice were cited from Table 2. (B) AUC ratios in 3aKO and hCYP3A/3aKO mice were cited from supplemental Table 1. Comparison of the two groups was made with Welch's t-test.

Metabolic disposition of triazolam and clobazam in humanized CYP3A mice with a double knockout background of mouse *Cyp2c* and *Cyp3a* genes

Kaoru Kobayashi, Genki Minegishi, Nina Kuriyama, Atsushi Miyajima, Satoshi Abe, Kanako Kazuki, Yasuhiro Kazuki

Drug Metabolism and Disposition

Manuscript Number: DMD-AR-2022-001087

Supplemental Table 1. AUC ratios of triazolam and its metabolites in WT, 3aKO and hCYP3A/3aKO mice.

Metabolite/triazolam	WT	3aKO	hCYP3A/3aKO
1'-hydroxytriazolam/triazolam	2.74 ± 0.789	0.528 ± 0.258**	0.428 ± 0.061**
4-hydroxytriazolam/triazolam	0.325 ± 0.058	0.050 ± 0.007**	0.086 ± 0.008**

Data are expressed as means ± S. D. (n = 5/group).

Mice were given an oral dose of triazolam (2 mg/kg). Plasma concentrations of triazolam, 1'-hydroxytriazolam and 4-hydroxytriazolam were determined and area under the plasma concentration-time curve (AUC₀₋₁₂₀) from 0 to 120 min was calculated using the linear trapezoidal method. **p<0.01 compared with WT (one-way ANOVA with a post-hoc test of Scheffé's F test).

Metabolic disposition of triazolam and clobazam in humanized CYP3A mice with a double knockout background of mouse *Cyp2c* and *Cyp3a* genes

Kaoru Kobayashi, Genki Minegishi, Nina Kuriyama, Atsushi Miyajima, Satoshi Abe, Kanako Kazuki, Yasuhiro Kazuki

Drug Metabolism and Disposition

Manuscript Number: DMD-AR-2022-001087

Supplemental Table 2. Primer list for genomic PCR analysis.

Gene or aim	Primer name (forward)	Forward primer (5'-3')	Primer name (reverse)	Reverse primer (5'-3')	Product size
Cyp2C KO junction	Cyp2c55 J1L	CACCAAAAGTCGATCTCTAGCCTCCACA	Cyp2c70 J1R	GTTGAGCTAGGCCTTGAGGAAACTCCAA	3 kbp
Cyp2c55	Cyp2c55 1L	AGCAGAACACACTGGCTGTTGC	Cyp2c55 1R	GACAGAGGATGGATCTGCATGG	191 bp
Cyp2c29	Cyp2c29 1L	TTTCTGGCCCCTGCTGTGAT	Cyp2c29 1R	TGTGTTTGCTGGGTCTTGAGAGA	128 bp
Cyp2c39	Cyp2c39 1L	AGATCACATATTCTGACCCCCTCCT	Cyp2c39 1R	CAGAAACCAGATGTGTTTGCTAGGTC	150 bp
Cyp2c54	Cyp2c54 1L	TCAAATGCCTGGCTCCACTG	Cyp2c54 1R	GGAATCAGGTCCATATCATCACAGC	192 bp

Metabolic disposition of triazolam and clobazam in humanized CYP3A mice with a double knockout background of mouse *Cyp2c* and *Cyp3a* genes

Kaoru Kobayashi, Genki Minegishi, Nina Kuriyama, Atsushi Miyajima, Satoshi Abe, Kanako Kazuki, Yasuhiro Kazuki

Drug Metabolism and Disposition

Manuscript Number: DMD-AR-2022-001087

Supplemental Table 3. Conditions used for LC-MS/MS analysis.

The LC-MS/MS system consisted of either Shimadzu LCMS8050 equipped with Nexera series HPLC system (System 1) or SCIEX QTRAP4500 equipped with a Shimadzu Prominence series HPLC system (System 2). Data from System 1 and 2 were processed using Lab Solution software (version 5.97 SP1, Shimadzu) and MultiQuant software (version 1.3, SCIEX), respectively. Mobile phases consisted of 0.1% formic acid in distilled water (Mobile phase 1), 0.1% formic acid in acetonitrile/methanol=1/1 (v/v) (Mobile phase 2), 10% methanol in distilled water (Mobile phase 3) and methanol (Mobile phase 4). The column was a COSMOSIL 3C18-MS-II (2.0 mm x 50 mm; Nacalai Tesque). Temperature of the autosampler and column was maintained at 4°C and 40°C, respectively.

Sample	drug	MRM transition	System	retention time (min)	Flow rate (ml/min) Time; rate	Injection volume (μL)	Mobile phase (A/B)	Gradient condition Time; B concentration	
incubation mixture	1'-hydroxytriazolam	359.3 > 176.1	1	1.92	0.6	1	1/2	0-0.6 min; 15%	
	4-hydroxytriazolam	359.3 > 314.0		1.93				0.6-2.0 min; 15%→90%	
	propranolol	260.1 > 116.2		1.59				2.0-3.8 min; 90%	
plasma	triazolam	343.0 > 308.1	2	2.40		5			3.8-3.81 min; 90%→15%
	1'-hydroxytriazolam	359.0 > 175.9		2.31					3.81-4.51 min; 15%
								0-2.0 min; 15%→90%	
								2.0-3.7 min; 90%	

	4-hydroxytriazolam	359.0 > 313.9		2.32				3.7-3.71 min; 90%→15%
	propranolol	260.1 > 116.0		1.89				3.71-5.0 min; 15%
plasma	CLB	301.1 > 259.3	1	3.30	0-2.4 min; 0.4→0.6 2.4-7.5 min; 0.6	2	3/4	0-1.0 min; 5%
	NCLB	287.1 > 245.2		3.23				1.0-2.4 min; 5%→98%
	oxazepam	287.1 > 241.2		3.35				2.4-7.0 min; 98% 7.0-7.01 min; 98%→5% 7.01-7.5 min; 5%

Metabolic disposition of triazolam and clobazam in humanized CYP3A mice with a double knockout background of mouse *Cyp2c* and *Cyp3a* genes

Kaoru Kobayashi, Genki Minegishi, Nina Kuriyama, Atsushi Miyajima, Satoshi Abe, Kanako Kazuki, Yasuhiro Kazuki

Drug Metabolism and Disposition

Manuscript Number: DMD-AR-2022-001087

Supplemental Table 4. Expression levels of mRNAs in the liver and intestine of WT, 3aKO, 2c3aKO, hCYP3A/3aKO and hCYP3A/2c3aKO mice.

	Genes	WT	3aKO	2c3aKO	hCYP3A/3aKO	hCYP3A/2c3aKO
Liver	CYP1A2	1.00 ± 0.05	0.90 ± 0.32	1.00 ± 0.18	0.80 ± 0.21	0.90 ± 0.25
	CYP2B10	1.00 ± 0.70	2.74 ± 1.39	12.46 ± 4.55 ^{**} , ^{††}	1.58 ± 0.53	4.90 ± 0.57 [§]
	UGT1A1	1.00 ± 0.12	1.31 ± 0.11	1.72 ± 0.09 [*]	1.86 ± 0.21 ^{**}	1.42 ± 0.38
	Mdr1a	1.00 ± 0.19	2.39 ± 0.78	5.94 ± 2.17 ^{**}	2.17 ± 0.18	2.49 ± 1.38
Intestine	CYP2B10	1.00 ± 0.19	0.80 ± 0.39	0.61 ± 0.16	0.26 ± 0.24	0.74 ± 0.26
	UGT1A1	1.00 ± 0.77	0.82 ± 0.21	0.85 ± 0.13	0.53 ± 0.51	0.85 ± 0.45
	Mdr1a	1.00 ± 0.78	1.70 ± 0.61	2.89 ± 0.64	0.99 ± 0.68	1.92 ± 0.86

The mRNA expression levels were normalized by expression levels of GAPDH mRNA. Data for each mouse (n = 3/group) are shown as means with S. D.

*p<0.05, **p<0.01 compared with WT, ^{††}p<0.01 compared with 3aKO, [§]p<0.05 compared with 2c3aKO (one-way ANOVA with a post-hoc test of Scheffé's F test).